Emission Spectroscopic Properties of the Red Form of Dichloro(2,2′-bipyridine)platinum(II). Role of Intermolecular Stacking Interactions

William B. Connick, Lawrence M. Henling, Richard E. Marsh, and Harry B. Gray*

Beckman Institute, California Institute of Technology, Pasadena, California 91125

Received May 9, 1996[⊗]

The structure of the red form of Pt(bpy)Cl_2 (bpy = 2,2′-bipyridine) has been studied by variable-temperature X-ray crystallography. The stack of square-planar Pt(bpy)Cl_2 units in the linear-chain material contracts with decreasing temperature; in the interval between 294 and 20 K, the platinum−platinum distance shortens from 3.449(1) to 3.370(2) Å. Both absorption and emission spectra of the red compound depend strikingly on temperature; as previously found for tetracyanoplatinate salts, the emission maximum red-shifts as the temperature drops (613 nm at 300 K; 651 nm at 10 K), with the peak energy decreasing linearly with the inverse cube of the metal−metal separation.

Introduction

Investigations of the spectroscopy of platinum(II) linear-chain systems have demonstrated that the maxima of the lowest energy absorption and emission bands display a strong dependence on the intrachain metal−metal separation.[1] A dramatic example is Pt(bpy)Cl_2 (bpy = 2,2′-bipyridine), which forms both yellow and red crystalline solids.[2−4] The Pt atoms are well separated in the yellow form (4.44 Å);[5−7] but in the red form, which is intensely luminescent (∼613 nm) even at room temperature,[4,8,9] the square-planar complexes stack to form an approximately linear Pt···Pt chain with a spacing of 3.45 Å.[10]

We have explored the role of intermolecular stacking interactions in tuning the spectroscopic properties of linear-chain platinum(II) complexes by examining the structure of the red form of Pt(bpy)Cl_2 over a wide temperature range. We found that the crystalline compound undergoes markedly anisotropic contraction with decreasing temperature; and, as established previously by Gliemann and Yersin for several tetracyanoplatinates,[1] the emission red-shifts systematically as the platinum atoms in the chain come closer together.

Experimental Section

Pt(bpy)Cl_2 was prepared according to the published protocol of Morgan and Burstall,[2] and crystals of suitable size for X-ray diffraction studies were grown by slow evaporation of a warm pyridine solution (∼50 °C). A small fragment (0.10 × 0.11 × 0.23 mm) was cut from a needle-shaped crystal and used for all crystallographic studies. Preliminary room-temperature data were collected on an Enraf-Nonius CAD4 diffractometer (Mo Kα radiation) with ω scans to a maximum 2θ value of 55° ($\pm h,\pm k,l$). The unit-cell dimensions were obtained from the setting angles of 25 reflections ($19° < 2\theta < 25°$). Throughout this study, diffraction data were corrected for Lorentz, polarization, and absorption (ψ scans of six reflections) effects; the intensities of three standard reflections showed no variations greater than those predicted by counting statistics.

Variable-temperature diffraction data were collected using a modified $P\bar{1}$ apparatus (Mo Kα radiation) designed by Samson and co-workers.[11] The temperature was cycled from 294 K (room temperature) to 20 K and back to room temperature; the unit-cell parameters were measured at several intermediate temperatures during both the descending and ascending phases of this cycle. The system was allowed to equilibrate for at least 3 h before making measurements; the temperature was typically stable to better than ±1 K. The unit-cell dimensions were determined at 294, 200, 100, and 20 K during the cooling phase and at 60, 100, 150, and 294 K during the warming phase; no hysteresis in the reflection intensities or unit-cell dimensions was observed. Cell dimensions were obtained from the setting angles of 28 reflections ($9.5° < \theta < 10.5°$), covering all eight octants.

Intensities ($\pm h,\pm k,\pm l$) were measured at three different temperatures: 294 K ($2\theta < 60°$), 200 K ($2\theta < 40°$), and 20 K ($2\theta < 81°$). In all cases, the systematic absences (hkl, $h + k = 2n + 1$; $h0l$, $l = 2n + 1$) were consistent with space groups *Cmcm* (No. 63), *Cmc*2_1 (No. 36), and *C*2*cm* (an alternative setting of *Ama*2, No. 40); the structures were successfully refined in the centrosymmetric *Cmcm*. In the case of the room-temperature data set, the Pt atom was located from a Patterson map and the positions of the remaining non-hydrogen atoms were found by successive structure factor and Fourier calculations. The resulting atomic positions were used as starting coordinates for the refinement of the structure at lower temperatures. Coordinates and anisotropic displacement parameters of all non-hydrogen atoms (as well as a scale factor and secondary extinction coefficient) were refined at all three temperatures; hydrogen atoms were positioned by calculation (C−H = 0.95 Å) after each cycle of refinement and were assigned isotropic B values 1.15 times those of the attached carbon atoms. Both real and imaginary parts of anomalous dispersion were used in all refinements. Two very strong, low-angle reflections (002 and 202) were deleted due to severe disagreement with the final model; these deviations may be symptomatic of uncorrected absorption effects and/or anisotropic secondary extinction. Weights were taken as $1/\sigma^2(F_o^2)$; variances $[\sigma^2(F_o^2)]$ were derived from counting statistics plus an additional term, $(0.014F_o^2)^2$; variances of the merged data were determined by propagation of esd's plus another additional term, $(0.014\langle F_o^2\rangle)^2$. Atomic scattering factors were taken from Cromer and Waber.[12,13] Computer programs used were those of the CRYM crystallographic computing

[⊗] Abstract published in *Advance ACS Abstracts,* September 15, 1996.

(1) Gliemann, G.; Yersin, H. *Struct. Bonding* **1985**, *62*, 87.
(2) Morgan, G. T.; Burstall, F. H. *J. Chem. Soc.* **1934**, 965.
(3) Miskowski, V. M.; Houlding, V. H. *Inorg. Chem.* **1989**, *28*, 1529.
(4) Houlding, V. H.; Miskowski, V. M. *Coord. Chem. Rev.* **1991**, *111*, 145.
(5) Textor, V. M.; Oswald, H. R. *Z. Anorg. Allg. Chem.* **1974**, *407*, 244.
(6) Canty, A. J.; Skelton, B. W.; Traill, P. R.; White, A. H. *Aust. J. Chem.* **1992**, *45*, 417.
(7) Herber, R. H.; Croft, M.; Coyer, M. J.; Bilash, B.; Sahiner, A. *Inorg. Chem.* **1994**, *33*, 2422.
(8) Weiser-Wallfahrer, M.; Gliemann, G. *Z. Naturforsch.* **1990**, *45B*, 652.
(9) Miskowski, V. M.; Houlding, V. H.; Che, C.-M.; Wang, Y. *Inorg. Chem.* **1993**, *32*, 2518.
(10) Osborn, R. J.; Rogers, D. *J. Chem. Soc., Dalton Trans.* **1974**, 1002.
(11) Samson, S.; Goldish, E.; Dick, C. J. *J. Appl. Crystallogr.* **1980**, *13*, 425.
(12) Cromer, D. T.; Waber, J. T. *International Tables for X-ray Crystallography*; Kynoch Press: Birmingham, U.K., 1974; Vol. IV, p 99.
(13) Cromer, D. T. *International Tables for X-ray Crystallography*; Kynoch Press: Birmingham, U.K., 1974; Vol. IV, p 149.

S0020-1669(96)00511-3 CCC: $12.00

Table 1. Crystallographic Data for Pt(bpy)Cl_2 at 294 and 20 K ($PtC_{10}H_8N_2Cl_2$, Orthorhombic, *Cmcm* (No. 63))

	294 K	20 K
a, Å	17.669(5)	17.598(10)
b, Å	9.081(2)	9.059(4)
c, Å	6.804(2)	6.643(3)
V, Å^3	1091.7(5)	1059.0(9)
D_{calc}, g/cm^3	2.57	2.65
Z	4	4
no. of reflns	880	1844
no. of reflns with $F_o^2 > 0$	868	1797
no. of reflns with $F_o^2 > 3\sigma(F_o^2)$	804	1714
no. of parameters	48	48
GOF[a]	1.74	2.19
R[b]	0.0326	0.0340
$R(F_o^2 > 3\sigma(F_o^2))$[b]	0.0289	0.0317

[a] GOF $= (\sum w(F_o^2 - F_c^2)^2/(n-p))^{1/2}$ where n is the number of data and p is the numberof parameters refined. [b] $R = \sum||F_o| - |F_c||/\sum|F_o|$.

Table 2. Final Positional Parameters ($\times 10^4$)[a] and Equivalent Isotropic Displacement Parameters (Å$^2 \times 10^4$, $U_{eq} = {}^1/_3\sum_j U_{ij} a_i^* a_j^* (\vec{a}_i \cdot \vec{a}_j)$) for Pt(bpy)$Cl_2$ at 294 and 20 K

atom	*T*, K	*x*	*y*	U_{eq}
Pt	294	0	−313(0.5)	261(1)
	20	0	−314(0.3)	32(1)
Cl	294	914(1)	−2119(3)	452(5)
	20	921(1)	−2127(1)	70(2)
N	294	732(3)	1380(7)	293(14)
	20	739(2)	1384(4)	47(7)
C(1)	294	1494(5)	1258(10)	455(22)
	20	1501(3)	1273(6)	93(7)
C(2)	294	1944(5)	2503(14)	623(29)
	20	1966(3)	2503(6)	91(8)
C(3)	294	1625(6)	3863(13)	646(30)
	20	1638(3)	3889(6)	94(8)
C(4)	294	850(6)	3974(10)	527(27)
	20	850(3)	4016(6)	84(7)
C(5)	294	408(4)	2729(9)	343(18)
	20	415(3)	2746(5)	66(9)

[a] The *z* coordinates are at ${}^1/_4$ by symmetry.

system,[14] ORTEP,[15] and THMA14.[16] Pertinent data are collected in Table 1, and final atomic positions and displacement parameters are summarized in Table 2.

Results and Discussion

Structure at 294 K. The room-temperature structure reported here and that reported earlier in a study by Osborn and Rogers[10] are in excellent agreement.[17] The unit-cell dimensions, measured three times in this study as well as once previously,[10] give average values with relatively small scatter standard deviations: $a = 17.669(5)$, $b = 9.085(3)$, $c = 6.802(2)$ Å. Our two room-temperature structures determined using data collected from two different diffractometers are identical within experimental error; thus, for simplicity, we restrict our discussion to the structure determined from the larger data set.

The neutral Pt(bpy)Cl_2 molecules lie at $z = {}^1/_4$ and $z = {}^3/_4$ and have crystallographic *mm*2 symmetry; the coordination geometry of the platinum is approximately square planar. A drawing of the molecule is shown in Figure 1a, and selected bond lengths and angles are given in Table 3. The crystal packing is illustrated in Figure 2; this arrangement of molecules results in stacking of the complexes to form a chain of planar Pt(bpy)Cl_2 units with a relatively short interplanar spacing of 3.402(1) Å (=c/2). The Pt atoms are displaced by 0.2843(4) Å along *b* from the chain axis (*c*), resulting in a Pt···Pt

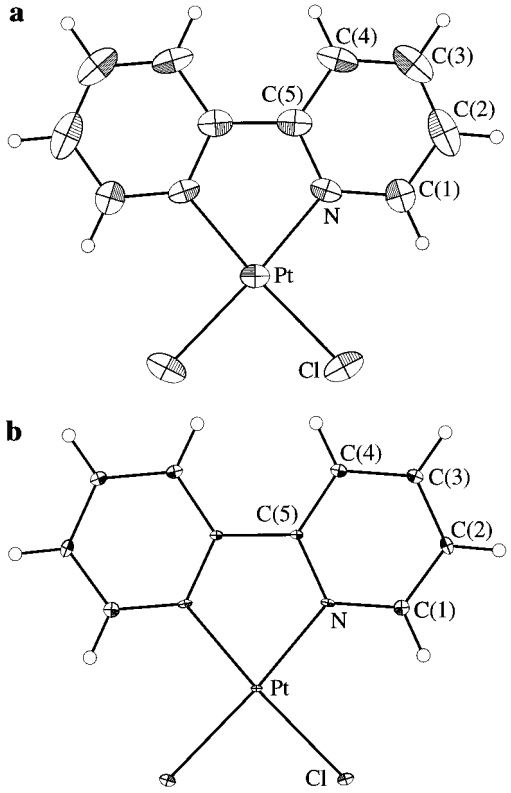

Figure 1. ORTEP[15] diagrams with 50% probability ellipsoids showing the geometry of the Pt(bpy)Cl_2 molecule at 294 K (a) and 20 K (b). H atoms are shown as spheres of arbitrary size.

Table 3. Bond Lengths (Å) and Angles (deg) for Pt(bpy)Cl_2 at 294 and 20 K[a]

	294 K	294 K (cor)	20 K
Pt−Cl	2.302(2)	2.310(2)	2.308(1)
Pt−N	2.009(6)	2.016(6)	2.015(4)
N−C(1)	1.350(10)	1.355(10)	1.343(6)
N−C(5)	1.352(10)	1.357(10)	1.360(6)
C(1)−C(2)	1.383(14)	1.388(14)	1.383(7)
C(2)−C(3)	1.358(15)	1.362(15)	1.382(7)
C(3)−C(4)	1.374(15)	1.379(15)	1.391(7)
C(4)−C(5)	1.373(12)	1.378(12)	1.382(7)
C(5)−C(5)′	1.442(11)	1.447(11)	1.459(6)
N−Pt−Cl	95.4(2)		95.2(1)
N−Pt−N′	80.2(2)		80.5(2)
N−Pt−Cl′	175.5(2)		175.6(1)
Cl−Pt−Cl′	89.1(1)		89.2(1)
Pt−N−C(1)	125.4(5)		125.9(3)
Pt−N−C(5)	114.9(5)		114.9(3)
C(1)−N−C(5)	119.8(7)		119.2(4)
C(2)−C(1)−N	120.5(8)		122.0(5)
C(3)−C(2)−C(1)	120.3(10)		119.0(5)
C(4)−C(3)−C(2)	118.8(10)		119.4(5)
C(5)−C(4)−C(3)	120.4(9)		118.9(4)
C(4)−C(5)−N	120.3(8)		121.5(4)
C(5)′−C(5)−N	115.1(7)		114.9(4)
C(5)′−C(5)−C(4)	124.6(8)		123.7(4)

[a] Primed atoms are related by a mirror plane: $-x, y, z$. Corrected 294 K distances were determined from a rigid-body analysis.[16]

(14) Duchamp, D. J. *Abstracts of Papers*, American Crystallographic Association Meeting, Bozeman, MT, 1964; No. B14, p 29.
(15) Johnson, C. K. ORTEPII. Report ORNL-5138; Oak Ridge National Laboratory: Oak Ridge, TN, 1976.
(16) Trueblood, K. N. *THMA14—Thermal Motion Analysis*; University of California: Los Angeles, CA, 1993.
(17) The most significant differences between our study and that previously reported[10] are an increased number of data, use of a $1/\sigma^2$ weighting scheme, refinement on F^2, and correction for secondary extinction; the last substantially improved agreement between the data and modeled structure.

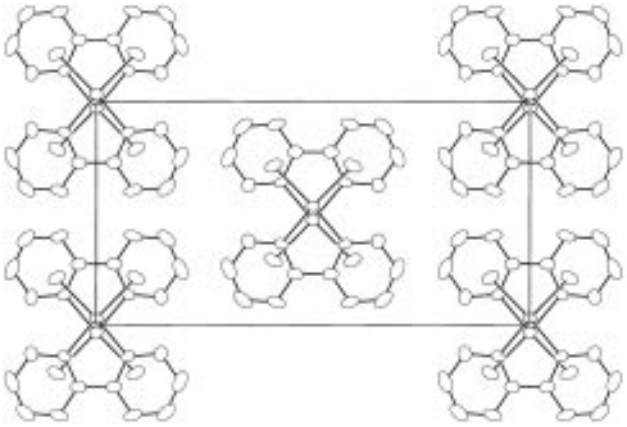

Figure 2. $Pt(bpy)Cl_2$ crystal packing at 294 K. View is along the *c* axis and perpendicular to the *ab* plane. H atoms are not shown.

separation between adjacent molecules of 3.449(1) Å and a Pt···Pt···Pt chain angle of 161.03(3)°.

The intramolecular distances and angles are in excellent agreement with those reported for the yellow form of $Pt(bpy)Cl_2$.[7] The Cl−Pt−Cl′ (89.1(1)°), N−Pt−N′ (80.2(2)°), and Cl−Pt−N′ (175.5(2)°) bond angles are within experimental error of those found for the yellow polymorph (89.1(1)°; 80.6(4)°; 175.9(3)°, 174.7(3)°).[7,18] Additionally, the Pt−Cl and Pt−N distances (2.302(2), 2.009(6) Å) are similar to those observed for the yellow form (Pt−Cl = 2.281(4), 2.300(3) Å; Pt−N = 2.006(10), 2.011(10) Å);[7] however, the Pt−N bond length is characteristically shorter than those reported for structures of complexes such as $Pt(bpy)(CN)_2$ (2.059(5) Å) that contain strong *trans* σ-donor/π-acceptor ligands.[19] The Pt−Cl distance is also nearly identical with values observed for $Pt(pyridine)_2Cl_2$ (2.291(5), 2.300(5) Å)[20] and Pt(5,5′-dimethyl-2,2′-bipyridine)Cl_2 (2.29 Å).[9,21] Similarly, the geometry of the bipyridyl ligand is in good agreement with that found for related compounds such as $Pt(bpy)I_2$.[22] Since the distances and angles in the red form accord with a number of platinum structures in which the Pt···Pt contacts are relatively long (>4.5 Å), the stacking interactions do not appear to perturb the molecular structure of the monomeric units.

Structure at 20 K. The molecular structure is essentially unchanged at lower temperatures, except for a gradual and slight elongation of the apparent bond lengths and substantially smaller mean-square atomic displacements; thus, we focus our discussion on the structure at the lowest temperature studied (20 K). A drawing of the molecule is shown in Figure 1b, and selected distances and angles are given in Table 3. On cooling, the bond lengths appear to expand by an average of 0.009(9) Å (scatter esd given in parentheses) with respect to the room-temperature values; this result is an example of the bond-shortening effect caused by larger librations at room temperature, as noted by Cruickshank.[23] A rigid-body analysis[16] of the room-temperature atomic displacement parameters indicates that the bonds should be lengthened by an average of 0.005(1) Å (Table 3), bringing them into much better agreement with the low-temperature values. Rigid-body corrections at 20 K are less than 0.001 Å.

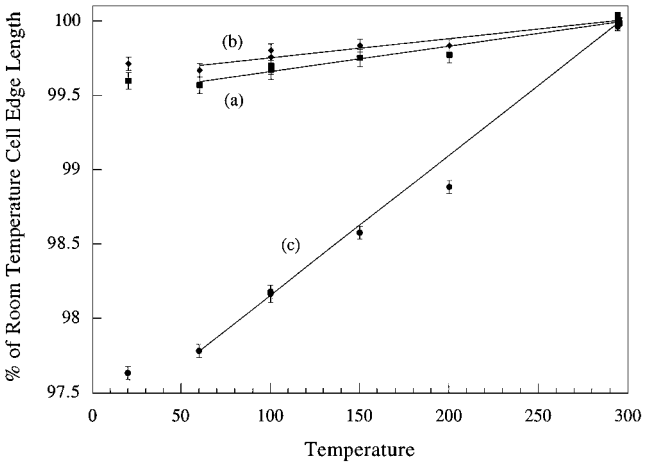

Figure 3. Cell edge length (*a*, *b*, and *c* axes) given as a percentage of the room-temperature average value plotted as a function of temperature. Linear fits of data from 295 to 60 K are also shown. The room-temperature measurement from ref 10 is included.

As expected, the atomic mean-square displacements (U_{ii}) are markedly reduced with decreasing temperature; the average ratio of the U_{eq} (equivalent isotropic mean-square displacement) at room temperature to the low-temperature value is 1.6(1) at 200 K and 6.4(10) at 20 K. The rigid-body analyses at all three temperatures confirm a gradual decrease in translational and librational molecular motion with decreasing temperature. Interestingly, at all temperatures there is distinct anisotropy in the U_{ii} for Pt (Figure 1); U_{11} (in-plane) and U_{33} (along the stacking direction) are substantially larger (approximately 3 times at 20 K) than U_{22} (in-plane, along refined coordinate of Pt). The rigid-body analyses support this observation; the mean-square displacements of translational motion (dominated by the Pt) are greater along the *a* and *c* axes than along the *b* axis by almost the same margin. We do not fully understand the reason for this anisotropy.

The most important change in the crystal structure with decreasing temperature is a substantial anisotropic contraction of the unit cell (Figure 3). When the crystal was cooled from room temperature to 20 K, the lengths of all three unit-cell edges decreased; no hysteresis was observed when the crystal was warmed to room temperature. In addition, there was no evidence of a phase transition over the temperature range studied, although such transformations have been observed in other platinum chain structures.[24,25] The length of the *c* axis exhibits the greatest thermal sensitivity, decreasing to 97.6% of the room-temperature value at 20 K; the corresponding unit-cell volume is 97.0% of the room-temperature volume. Assuming a linear dependence of thermal expansion over the temperature range from 295 to 60 K (Figure 3), the estimated expansion coefficient along *c* of $9.4(3) \times 10^{-5}$ K^{-1} at 295 K is substantially larger than that found along the *a* ($1.7(1) \times 10^{-5}$ K^{-1}) and *b* ($1.3(1) \times 10^{-5}$ K^{-1}) axes.[26] The coefficient of linear

(18) In ref 7 the *trans*-Cl−Pt−N angles were reported to be significantly different for the red and yellow forms of $Pt(bpy)Cl_2$. Using the coordinates reported by Osborn and Rogers,[10] the authors calculated a value of 184° for the red form; in fact, this result (=360° − 176°) is in good agreement with the values reported for the yellow form (175.9(3), 174.7(3)°).

(19) Connick, W. B.; Henling, L. M.; Marsh, R. E. *Acta Crystallogr.*, in press.

(20) Colamarino, P.; Orioli, P. L. *J. Chem. Soc., Dalton Trans.* **1975**, 1656.

(21) In ref 9 the structure of Pt(5,5′-dimethyl-2,2′-bipyridine)Cl_2 was described in space group *Cc* (No. 9). Taking into account the presence of a 2-fold symmetry axis bisecting the molecule, centrosymmetric *C*2/*c* (No. 15) is a more appropriate choice of space group; some of the earlier reported distances may be unreliable.

(22) Connick, W. B.; Gray, H. B. *Acta Crystallogr.* **1994**, *C50*, 1040.

(23) Cruickshank, D. W. J. *Acta Crystallogr.* **1956**, *9*, 757.

(24) Daniels, W.; Yersin, H.; von Philipsborn, H.; Gliemann, G. *Solid State Commun.* **1979**, *30*, 353.

(25) Yersin, H.; Gliemann, G.; Räde, H.-S. *Chem. Phys. Lett.* **1978**, *54*, 111.

(26) The coefficient of linear thermal expansion is given by $(1/s)(\partial s/\partial T)$, where *s* is the unit-cell edge length at a given temperature.

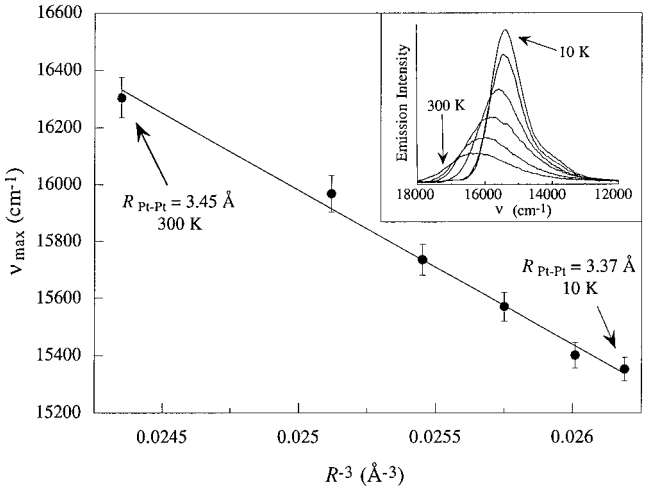

Figure 4. Emission peak energy (ν_{max}) as a function of the inverse cube of the Pt···Pt separation (R^{-3}). The linear fit corresponds to eq 2. Error bars are estimated standard deviations. Inset (adapted from ref 4) shows six emission spectra of the red form of $Pt(bpy)Cl_2$ (the bands red-shift from 300 to 10 K; intermediate temperatures are 200, 150, 100, and 50 K).

thermal expansion of platinum metal is only 0.9×10^{-5} K^{-1} at 298 K.[27] However, highly anisotropic thermal expansion is characteristic of both palladium[28] and platinum linear-chain materials,[1] and measured expansion coefficients along the stacking axis of tetracyanoplatinate salts range from 8×10^{-5} to 15×10^{-5} K^{-1} at 295 K.[1]

The cooling-induced contraction of the *c* axis is accompanied by a shortening of the intermolecular contacts between stacked complexes. As there is almost no slippage of the molecules in the *a* or *b* direction with decreasing temperature, the interplanar spacing between stacked $Pt(bpy)Cl_2$ units matches the contraction of *c* with decreasing temperature. Thus, at 20 K, the intermolecular spacing of 3.322(2) Å (=*c*/2) and the Pt···Pt distance of 3.370(2) Å are significantly shorter than the room-temperature values of 3.402(1) and 3.449(1) Å. The corresponding Pt···Pt···Pt chain angle of 160.59(4)° is approximately 0.4° smaller than at room temperature. Accounting for the small temperature dependence of the Pt *y* coordinate, the Pt···Pt separation was estimated at temperatures for which only unit-cell data are available. The resulting data were fit to a quadratic equation expressing the temperature (*T*) dependence of the Pt···Pt separation (*R*) between 20 and 294 K:

$$R_{Pt\cdots Pt} = 3.3657 + 0.000170T + 3.72 \times 10^{-7}T^2 \quad (1)$$

where *R* and *T* are in units of Å and K, respectively. Analysis of EXAFS (extended X-ray absorption fine structure) spectra measured at 110 K gave 3.37 ± 0.01 (or 3.36 ± 0.02) Å for the Pt···Pt distance;[7] for comparison, the predicted value at this temperature (eq 1) is 3.389 Å.

Emission (300−10 K). The temperature dependence of the emission spectrum of the red form of crystalline $Pt(bpy)Cl_2$ is striking (inset of Figure 4).[3,8,9] At room temperature, there is a relatively narrow (2000 cm^{-1} fwhm) and asymmetric band with a maximum at 613 nm (16 300 cm^{-1}); with decreasing temperature, this band sharply narrows and red-shifts, and at 10 K, the peak is at 651 nm (15 350 cm^{-1}; 1050 cm^{-1} fwhm). In addition, a distinctive shoulder is resolved approximately 1500 cm^{-1} further to the red of the 15 350 cm^{-1} peak at 10 K; vibronic structure with this spacing is diagnostic of involvement of the bipyridyl ligand in the electronic transition.[9] Interestingly, in the single-crystal polarized absorption spectrum, the lowest energy feature also shows a marked temperature dependence, strongly red-shifting (~1100 cm^{-1}) as the temperature is lowered from 298 to 10 K; a vibronic feature approximately 1500 cm^{-1} to higher energy exhibits similar behavior.[8] These observations suggest that the emissive state is ^{3}MLCT [dσ^* → π^*(bpy)], where the HOMO (dσ^*) derives from the interaction of the d_{z^2}(Pt) orbitals of the stacked complexes and the LUMO (π^*) is predominantly centered on the bipyridyl ligand. In accord with the triplet (^{3}MLCT) assignment, the lifetime of the emission from a solid sample of red $Pt(bpy)Cl_2$ is 155 ns at room temperature.[4,9]

Lattice contraction enhances the electronic coupling between stacked $Pt(bpy)Cl_2$ units; as the temperature is lowered from 294 to 20 K, there is a 0.08 Å shrinkage of the Pt···Pt distance, resulting in a smaller dσ^*−π^*(bpy) energy gap. In Figure 4, the emission peak energies[4,9] at temperatures from 300 to 10 K are plotted as a function of R^{-3}, where *R* has been estimated using eq 1.[29] The emission maximum (ν_{max}) exhibits an approximately linear dependence on R^{-3}; in eq 2, ν_{max} is in

$$\nu_{max} = 29.5(55) \times 10^3 - 5.4(3) \times 10^5 R^{-3} \quad (2)$$

cm^{-1}, *R* is in Å, and estimated standard deviations are given in parentheses. This linear relationship is reminiscent of the correlation between the emission energy and R^{-3} found for stacked $Pt(CN)_4^{2-}$ complexes with *R* values from 3.7 to 3.1 Å.[1,30−32] The value of ν_{max} as $R \rightarrow \infty$ corresponds to the electronic transition d$\sigma^* \rightarrow \pi^*$(bpy) in the absence of inter-complex electronic coupling—that is, the transition to the ^{3}MLCT [d_{z^2}(Pt) → π^*(bpy)] state in the monomer.[33] The uncertainty in the predicted $\nu_{monomer}$ value is large since the range of measured *R* values is relatively narrow in this system (3.45−3.37 Å); nevertheless, the value for $Pt(bpy)Cl_2$ is well below the $\nu_{monomer}$ estimates obtained from analysis of the tetracyanoplatinate linear-chain data (36 800 cm^{-1}, **E**⊥**c**; 42 900 cm^{-1}, **E**||**c**).[1] This difference is not unexpected, since the emissions in these two systems originate from different excited states; in the case of tetracyanoplatinate linear chains, there are two emissive levels, a singlet and a triplet,[1] and both are predominantly metal-centered d$\sigma^* \rightarrow$ pσ states.

The linear relationship between the ^{3}MLCT emission peak position and R^{-3} for $Pt(bpy)Cl_2$ is a reflection of the strong dependence of the dσ^* energy on metal−metal separation. In the case of stacked $Pt(CN)_4^{2-}$ units, extended Hückel calculations predict the observed dσ^*−pσ band-gap dependence on

(27) Weast, R. C., Ed. *Handbook of Chemistry and Physics*, 66th ed.; CRC Press, Inc.: Boca Raton, FL, 1985.
(28) Kistenmacher, T. J.; Destro, R. *Inorg. Chem.* **1983**, *22*, 2104.
(29) Values of *R* at 10 and 300 K were obtained from extrapolation of eq 1; as the coefficient of thermal expansion is expected to decrease at low temperature, the Pt···Pt separation at 10 K may be somewhat underestimated.
(30) Day, P. *J. Am. Chem. Soc.* **1975**, *97*, 1588.
(31) Yersin, H.; Gliemann, G. *Ber. Bunsen-Ges. Phys. Chem.* **1975**, *79*, 1050.
(32) Yersin, H.; Gliemann, G.; Rössler, U. *Solid State Commun.* **1977**, *21*, 915.
(33) The assignment of the monomer ^{3}MLCT [d_{z^2}(Pt) → π^*(bpy)] transition in the solution absorption spectrum of $Pt(bpy)Cl_2$ is complicated by the presence of intense charge-transfer features in this region. Nevertheless, the predicted $\nu_{monomer}$ is higher than the energy of the lowest ^{1}MLCT absorption band ($\nu_{max} \cong$ 25 400 cm^{-1}) in CH_2Cl_2 solution (Gidney, P. M.; Gillard, R. D.; Heaton, B. T. *J. Chem. Soc., Dalton Trans.* **1973**, 132); this result is consistent with the expected ($z^2 < xz, yz$) ordering of occupied d orbitals in a PtN_2X_2 complex (Martin, D. S. In *Extended Linear Chain Compounds*; Miller, J. S., Ed.; Plenum Press: New York, 1982; Vol. 1, pp 409−448).

R^{-3}.[34] These calculations,[32,35] as well as studies of d^8-d^8 dimers,[36] indicate that the energy of the HOMO ($d\sigma^*$) is considerably more sensitive to metal−metal separation than is the energy of the LUMO ($p\sigma$). Indeed, the slope ($-5.4(3) \times 10^5$ Å^3 cm^{-1}) of the fitted line in Figure 4 is slightly less steep than that found for the tetracyanoplatinate linear chains (-6.3×10^5 Å^3 cm^{-1}, **E**⊥**c**, triplet; -8.0×10^5 Å^3 cm^{-1}, **E**||**c**, singlet).[1] Reported[8] polarized emission maxima for the red form of $Pt(bpy)Cl_2$ at 20 and 298 K also suggest a slightly weaker dependence on metal−metal separation (based on a two-point determination of slope: -5×10^5 Å^3 cm^{-1}, **E**⊥**c**; -6×10^5 Å^3 cm^{-1}, **E**||**c**); similarly, from 10 to 298 K, the lowest energy feature in the polarized single-crystal absorption spectrum of $Pt(bpy)Cl_2$ apparently exhibits a weaker Pt···Pt dependence (two-point determination: -6×10^5 Å^3 cm^{-1}, **E**⊥**c**) than found for the $Pt(CN)_4^{2-}$ chains (-8.0×10^5 Å^3 cm^{-1}, **E**⊥**c**).[1] It is likely that the R dependence of the $d\sigma^*$ energy is weaker in the $Pt(bpy)Cl_2$ chains, owing to the smaller extension of the d_{z^2}(Pt) orbital in the neutral molecule relative to that in the negatively charged $Pt(CN)_4^{2-}$ complex. It also is possible that the $Pt(bpy)Cl_2$ π^*(bpy) energy is less sensitive than the $Pt(CN)_4^{2-}$ $p\sigma$ energy to metal−metal separation.

(34) An exciton-coupling description of tetracyanoplatinate spectra also predicts the observed R^{-3} dependence, assuming simple dipole−dipole coupling and only nearest-neighbor interactions.[30] In this model, the slope is proportional to the transition dipole moment, which is in turn proportional to the electronic transition oscillator strength. Indeed, the oscillator strength of the $d\sigma^* \rightarrow \pi^*$ ^{1}MLCT transition in face-to-face dimers of Pt(diimine) complexes (Bailey, J. A.; Miskowski, V. M.; Gray, H. B. *Inorg. Chem.* **1993**, *32*, 369. Connick, W. B.; Miskowski, V. M.; Gray, H. B. Unpublished results) is weaker than that of the $d\sigma^* \rightarrow p\sigma$ transition of $Pt_2(P_2O_5H_2)_4^{4-}$ (Stiegman, A. E.; Rice, S. F.; Gray, H. B.; Miskowski, V. M. *Inorg. Chem.* **1987**, *26*, 1112).

(35) Whangbo, M.-H.; Hoffmann, R. *J. Am. Chem. Soc.* **1978**, *100*, 6093.

(36) Smith, D. C.; Miskowski, V. M.; Mason, R. W.; Gray, H. B. *J. Am. Chem. Soc.* **1990**, *112*, 3760.

Acknowledgment. We thank K. I. Hardcastle, V. M. Miskowski, and V. Schomaker for helpful discussions and expert technical assistance. This work was supported by the NSF.

Supporting Information Available: Tables giving complete crystallographic experimental details, distances and angles, positional parameters for all atoms, and additional ORTEP unit-cell diagrams, anisotropic displacement parameters, and a plot of the Pt···Pt separation vs temperature (19 pages). Ordering information is given on any current masthead page.

IC960511F